scientific reports

OPEN

Regime shift of skeletal δ^{13}C after 1997/1998 El Nino event in *Porites* coral from Green Island, Taiwan

Masataka Ikeda[1], Atsuko Yamazaki[2,3], Kazuto Ohmori[4], Hong-Wei Chiang[5], Chuan-Chou Shen[5,6] & Tsuyoshi Watanabe[2,7,8✉]

The 1997/1998 El Niño event caused mass coral bleaching and mortality in many tropical and subtropical regions, including corals on Green Island, Taiwan, in the northwestern Pacific Ocean. This study analyzed coral carbon isotope ratios (δ^{13}C), oxygen isotope ratios (δ^{18}O), and Sr/Ca ratios for 29 years, including the 1997/1998 El Niño period, to examine how high water temperature events are recorded in coral geochemical indicators. Sr/Ca ratios in coral skeletons from Green Island show the lowest peak, means the highest temperature during the 1997/1998 El Niño period. However, we couldn't observe high-temperature events on δ^{18}O. Furthermore, a negative δ^{13}C shift was observed after El Niño events. The regime shift of δ^{13}C might have been caused by temporal bleaching and/or a decrease in symbiotic algae due to high water temperature stress under the continuous decrease in δ^{13}C in DIC due to the Suess effect.

The El Niño-Southern Oscillation (ENSO) is one of the most thermal stressors for corals and has become more frequent and severe in recent decades[1]. The regions that experienced the high sea surface temperature (SST) associated with the 1997/1998 El Niño event faced mass coral bleaching and mortality[2]. However, a few weeks of bleaching events can only be confirmed by visual inspection at various locations, making it difficult to know the occurrence of past bleaching events. Annual bands of reef-building coral skeletons have been used as paleoenvironmental archives. If a proxy of bleaching events can be found, it will be possible to reconstruct past bleaching records continuously.

Bleaching is the reduction or complete withdrawal of symbiotic algae from corals, leading to starvation, emaciation, disease, and death due to reduced nutrient availability from the symbionts[3]. To compensate for the lack of photosynthetic energy, reef-building corals use stored energy[4–8], increased heterotrophic feeding[6], decreased metabolic rates[8], decreased calcification rates[9,10]. The long-lived massive corals are alive as their aragonite skeletons form with aragonite, and their skeletons have recorded their responses to thermal stress events. In coral skeletal growth, abrupt decreases in annual extension rates, high-density stress bands[9–11], and growth hiatuses due to partial mortality[11–13] have been reported. Although many factors vary coral skeletal δ^{13}C, δ^{13}C in seawater[14], δ^{13}C of the metabolic CO_2[15], amount of solar radiation[16], vital effects[17], kinetic isotope fractionation[18,19] and spawning[20], the previous studies have reported the δ^{13}C in the coral skeletons decreased after the 1997/1998 El Niño event[21–24]. Coral skeletal stable oxygen isotope (δ18O) is a proxy for SST and seawater δ^{18}O[18]. Still, a negative shift has been reported following the 1997/1998 El Niño, associated with reduced coral extension rates[13].

Coral skeletal Sr/Ca ratios are used as reliable SST proxy[25], but anomalies of Sr/Ca have been reported during El Niño event[13,26–28]. Trace element (TE) uptake into coral skeletons might be affected by changes in skeletal microstructure[29–31]. For example, it causes a reduction in calcification rate due to heat stresses decreasing $Ca2+$ transport by the Ca-ATPase pump and causing changes in TE/Ca in the skeleton[32–34]. As a result, Sr/Ca is expected to be larger than that is expected from SST[35].

There is still no unified view on how bleaching events are recorded in coral skeletons, and many research cases are needed. In this study, we analyzed δ^{13}C, δ^{18}O, and Sr/Ca ratios in Porites coral cores from Green Island,

[1]Institute for the Advancement of Higher Education, Hokkaido University, Sapporo, Japan. [2]KIKAI Institute for Coral Reef Sciences, Kikai Town, Japan. [3]Graduate School of Environmental Studies, Nagoya University, Nagoya, Japan. [4]Hokkaido Research Organization (Environmental and Geological Research Department, Geological Survey of Hokkaido), Sapporo, Japan. [5]High-Precision Mass Spectrometry and Environment Change Laboratory (HISPEC), Department of Geosciences, National Taiwan University, Taipei, Taiwan ROC. [6]Research Center for Future Earth, National Taiwan University, Taipei, Taiwan. [7]Department of Natural History Sciences, Faculty of Science, Hokkaido University, Sapporo, Japan. [8]Research Institute for Humanity and Nature, Kyoto, Japan. ✉email: nabe@sci.hokudai.ac.jp

Taiwan, where coral bleaching events were reported with 1997/1998 El-Nino, to determine how high-water temperature events are recorded in coral geochemical indices.

Materials and methods
Study sites and samples

We drilled coral cores from a massive Porites colony alive at Green Island off the southeast coast of Taiwan on the 7th of April 2009. Green Island (Lutao) belongs to the tropical region in Taiwan and is located on the north of Kuroshio bifurcation, and the current speed is rapidly flowing northward[36]. Underwater coral drilling was performed at a depth of 12 m off the west coast of Green Island (22°39'231 N, 121°28'342E, Fig. 1) using an underwater drilling system. The coral cores are 8 cm in diameter and 2 m long. The coral tissue on the core top was soaked overnight in household bleach (HClO diluted to about 0.1% with water). Cores were sliced along the axis of maximum coral growth. After rinsing with Milli-Q water, they were dried. X-ray photographs were taken (Fig. 2) using a non-destructive transmission 2D X-ray imaging scanner TATSCAN-X1[37] at 37.6 or 38.6 kV with an exposure of 2.02 mA. The X-ray images were used to identify the annual density bands and determine the measurement lines of geochemical analysis.

The 2 mm thick ledges were formed along each measurement line. To remove cutting dust, the ledges were ultrasonically cleaned three times for 10 min in distilled water and completely dried at 30 °C. 1365 powder samples were collected at 1 mm intervals and 2 mm widths along the maximum growth lines using the micro-sampling method with a micro drill and a digitally controlled automated stage.
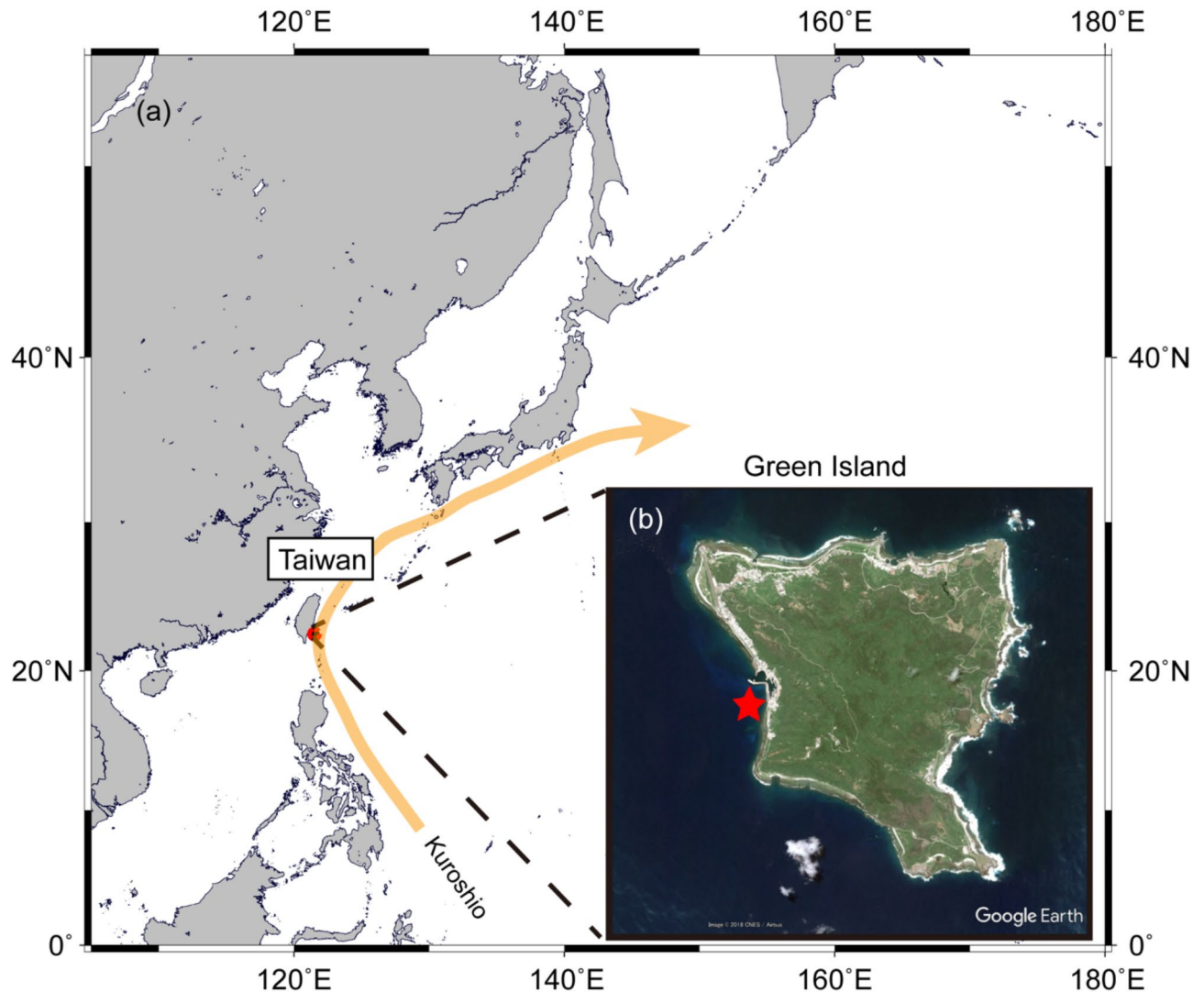
Fig. 1. The location of Green Island in Taiwan (photo by Google earth) showing (**a**) north-east Pacific, (**b**) Green Island. A star indicates a sampling site.
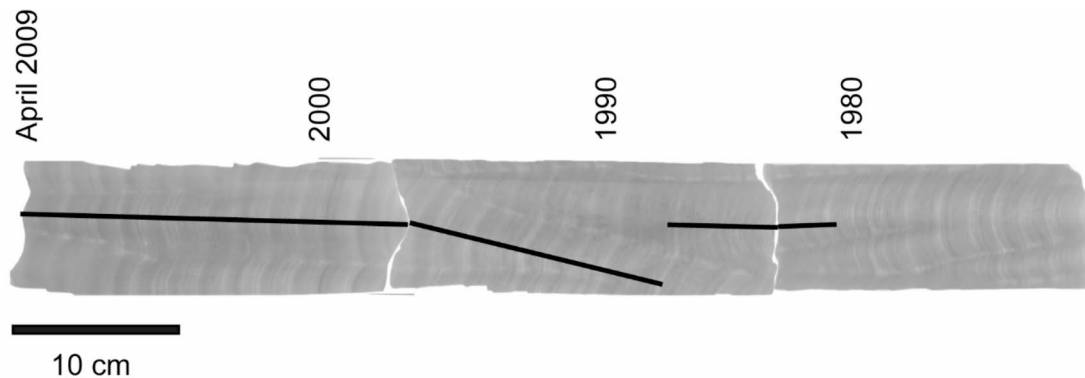
Fig. 2. The X-ray photographs of the coral core slabs. The black lines are the tracks of geochemical analysis.

Geochemical analysis

The $\delta^{18}O$ and $\delta^{13}C$ in coral skeletal powder were analyzed using a Finnigan MAT251 stable isotope ratio mass spectrometer system connected to an automated individual-carbonate device (Finnigan; Kiel Device II). The carbonate powder was reacted with 100% H_3PO_4 at 70 °C in the Kiel Device II and the resulting CO_2 gas produced was induced in the MAT251. The isotopic δ-values with Vienna Pee Dee Belemnite (VPDB) scale derived from stable isotope ratios were obtained from duplicate measurement of NBS19 standard (IAEA certified values; $\delta^{18}O$ = − 2.20‰, $\delta^{13}C$ = + 1.95‰). Standard deviations (1σ) of the duplicate analysis of NBS19 were 0.11‰ and 0.07‰ for the coral $\delta^{18}O$ and $\delta^{13}C$, respectively.

Sr/Ca ratios in coral skeletal powder were determined by inductively coupled plasma atomic emission spectroscopy (ICP-AES, Thermo Fisher Scientific; iCAP6200) following a combined method of Schrag[38], de Villiers et al.[39]. and Watanabe et al.[40]. After dissolving the sample powder in 0.5 ml of 25% HNO_3, the solution was diluted with Milli-Q to Ca concentrations of 7 mg/L and analyzed by ICP-AES connected to an automatic sampler (CETAC; ASX-260). All data were calibrated against JCP-1[41] solution using Ca concentrations of 7 mg/L as standard. The analytical errors (RSD) were 0.181% for the coral Sr/Ca.

Age model and statistical analysis

Sr/Ca ratios compared with annual density bands were used to construct age models for all other proxies. A Sr/Ca cycle represents one year; the maximum (minimum) Sr/Ca value was associated with the minimum (maximum) SST record. Proxy data were resampled to 12 data per year using AnalySeries software ver.2.0.8[42]. A regime shift of the proxies was tested by following Rodionov[43].

SST data and NINO 3.4 index

To compare the isotopic data and Sr/Ca data, SSTs for the sample site were derived from the "Advanced Very High Resolution Radiometer (AVHRR)[44]" satellite dataset on the National Oceanic and Atmospheric Administration (NOAA) of Integrated Global Ocean Services System (IGOSS). The dataset is a 1°×1° grid, covering 29 years from 1980 to 2010 over 22° N − 23° N, 121° E − 122° E. The NINO3.4 index was calculated using SST data from 1981 to 2010. The NINO 3.4 index was normalized to the 1981–2010 ERSST.v5 anomaly for the NINO 3.4 region (5° N–5° S, 12° W–170° W) from Climate Explorer at the Royal Netherlands Meteorological Institute (KNMI)[45]. The maximum SST was 31.5 °C in August 1998, and the minimum was 21.2 °C in March 1987.

Results

Coral Sr/Ca ratios show 27 clear annual cycles from 1983 to 2009 (Fig. 3). Sr/Ca ratios range from 8.51 mmol/mol to 9.21 mmol/mol with an average of 8.94 mmol/mol. The lowest peak of Sr/Ca ratios corresponded with the highest temperature anomaly of the SST in 1997/1998. The regime shift was observed before and after 1997 with the regime shift test, which showed the average of Sr/Ca ratios decreased from 8.96 mmol/mol to 8.92 mmol/mol. The coral Sr/Ca-SST relationship obtained from the linear regression of the monthly Sr/Ca and SST records.

$$\mathrm{Sr/Ca} = -0.050 \ (\pm 0.0035) \times \mathrm{SST} \ (^{\circ}C) + 10.253 \ (\pm 0.351) \ (R^2 = 0.79, \ n = 330) \tag{1}$$

Coral $\delta^{18}O$ also shows annual cycles as Sr/Ca ratios (Fig. 3). The fluctuations of $\delta^{18}O$ ranged from − 6.00‰ to − 4.26‰ with an average of − 5.21‰ (Fig. 3). The coral $\delta^{18}O$ was negatively shift of − 0.29‰ before and after 2006. The coral $\delta^{18}O$-SST relationship between the monthly coral $\delta^{18}O$ and SST was:

$$\delta^{18}O = -0.186 \ (\pm 0.008) \times \mathrm{SST} \ (^{\circ}C) - 0.25 \ (\pm 0.52) \ \left(R^2 = 0.92, \ n = 330\right) \tag{2}$$

Coral $\delta^{13}C$ shows clear annual cycles ranging from − 4.48‰ to − 1.52‰ with an average of − 3.02‰ (Fig. 4). With the regime shift test, the two shifts were observed in the 1987 and 1997/1998 El Niño years with decreases in the time series of $\delta^{13}C$ through the 27 years. The mean $\delta^{13}C$ values were − 2.47‰ from 1982 to 1986, − 2.90‰
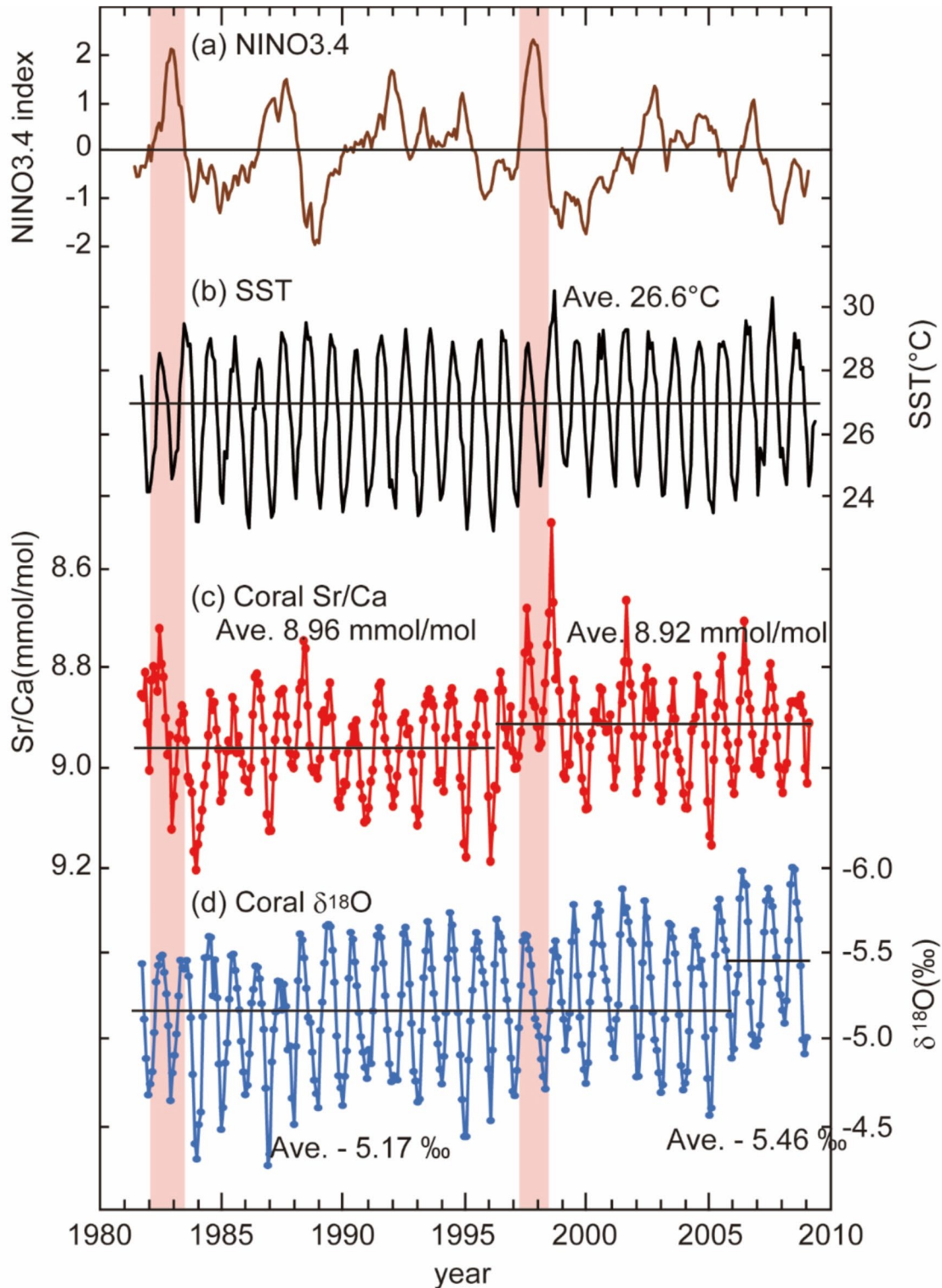
Fig. 3. SST from AVHRR for 1986–2009 including 1997/1998 El Niño event (**a**). Records of Sr/Ca ratio (**b**) and δ18O (**c**) in coral skeletons.

from 1986 to 1996, and − 3.31‰ from 1996 to 2010. After the 1997/1998 El Niño, the mean of the maxima shifted by − 0.60‰ and the mean of the minima by − 0.37‰.

The coral annual extension rates estimated from the Sr/Ca ratios and density bands varied from 13 to 21 mm/ year, with an average of 18 mm/year (Fig. 4).
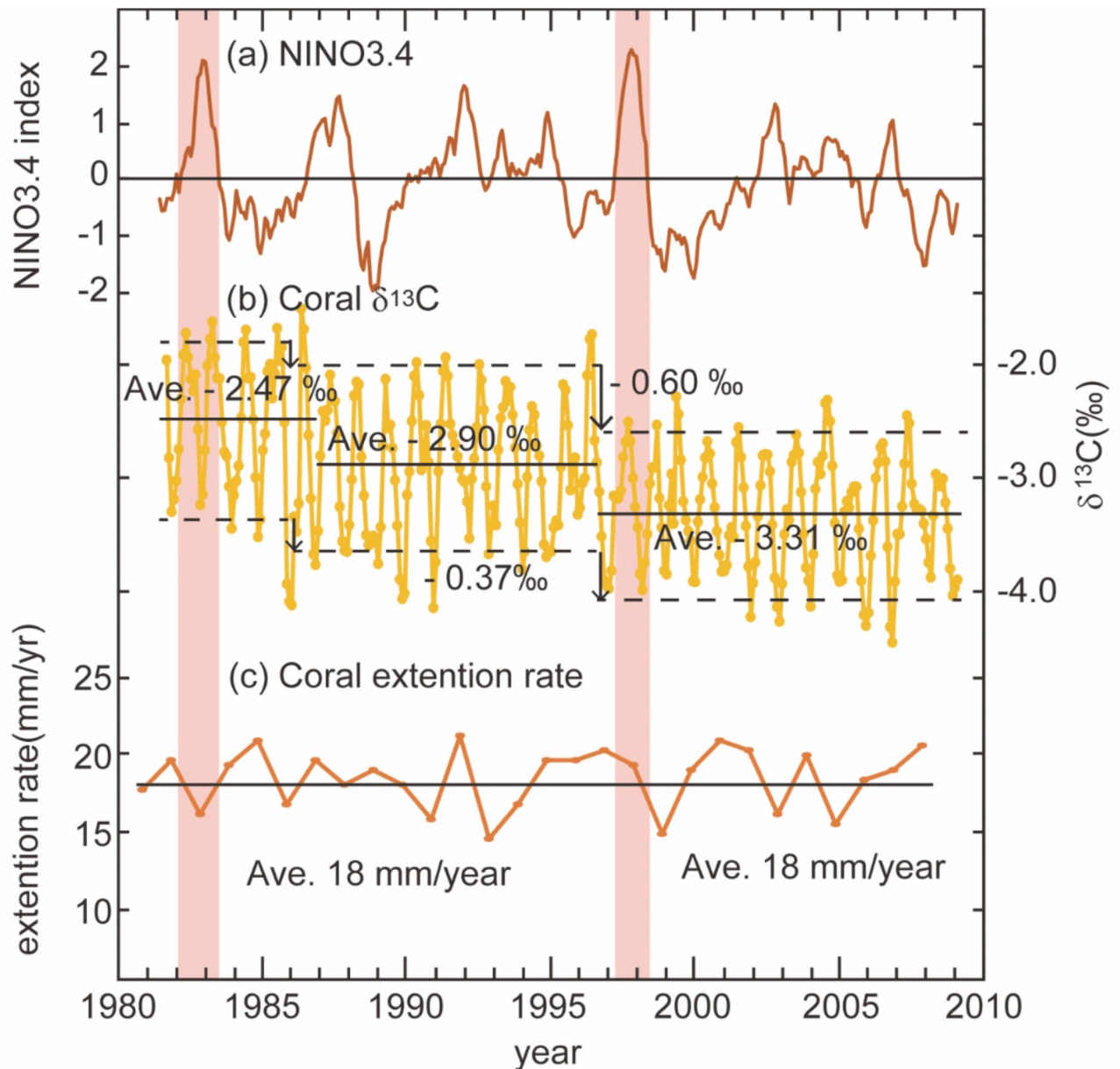
Fig. 4. Comparison of NINO3.4 index (**a**) including 1997/1998 El Niño event with records of $\delta^{13}C$ (**b**), and the coral extension rate (**c**). Black solid lines show averages in each period and broken lines show averages of maximum and minimum in each year. The solid black lines show the average of the respective periods before and after 1997/1998 El Niño, and the dashed lines show the average of the maximum and the minimum values for each year. The hatched areas represent the 1997/1998 El Niño seen from NINO3.4 index. The red hatched areas represent the particularly large 1981/1982 and 1997/1998 El Niño which NINO3.4 index indicates more than 2.

Discussion

During the 1997/1998 El-Nino event, coral Sr/Ca showed apparent high-temperature anomalies consistent with the SST data, while $\delta^{18}O$ showed no anomalies. Sr/Ca shifted negatively and maintained lower average values, and this trend is observed in other trace elements (Fig. S2; Mg/Ca). The changes in concentration of trace elements with El Niño events have been reported in previous studies[13,26–28]. Without the term of El Nino, Sr/Ca and $\delta^{18}O$ maintained a linear relationship with SST. Shen et al.[46] reported a slope range of − 0.051 to − 0.053 mmol/mol for the Sr/Ca-SST relationship for Porites in southern Taiwan, and the slope obtained from Eq. (1) is consistent with previous studies. The slope of the linear relationship of the coral $\delta^{18}O$-SST is − 0.186 from − 0.186 to −0.209‰, which aligns with previous studies in the Pacific Ocean[37,47–49].

Several factors may be responsible for decreased coral $\delta^{13}C$ observed in 1986–1988 and 1997/1998 El Niño. While an accelerated decrease in $\delta^{13}C$ reflecting the accumulation of anthropogenic CO_2 in the surface ocean is well known (i.e., the Suess effect)[50], the stepwise decrease in coral skeletons associated with the El Niño event in

this study could not be only consistent with the continuous trend of the Suess effect. The negative regime shift in the coral δ^{13}C after each El Niño event is similar to that reported by Wang et al.[21] from South China Sea. They proposed three possibilities of decline for δ^{13}C: a decrease in zooxanthellae density, an exchange to the different species of zooxanthellae with stronger thermal tolerance before and after the stepwise change of δ^{13}C, and a kinetic effect[21].

The coral physiological changes due to thermal stress with the density of zooxanthellae could be decline coral δ^{13}C. The δ^{13}C differences between unbleached and bleached corals, that an 85% loss of symbiotic algal density in bleached corals, were reported $-0.4\sim-1\permil$[7]. The coral δ^{13}C decline in this study, -0.37 and $-0.60\permil$ for 1986–1988 and 1997/1998 El-Nino, is within the range of coral δ^{13}C decline with bleaching events.

The stepwise decrease in coral δ^{13}C may be due to multiple factors resulting from El Niño or decadal-scale climate change and long-term variations such as the Suess effect. The exchanging of different zooxanthellae species might maintain average coral δ^{13}C afterward. The reconstruction of symbiosis between coral-algae with mass breaching events have been reported[51]. However, it has been reported that Porites corals have less diversity of symbiodinium species[52]. The possibility of change in coral δ^{13}C due to symbiodinium species has room for demonstration for future studies. McConaughey[18,19] suggested that slowing coral skeletal growth makes δ^{13}C increase due to kinetic effects. However, the extension rates of the coral in this study did not change after El Niño. The coral δ^{13}C decreasing is not explained by the kinetic effect with thermal stress event in this study.

In other previous studies, the stepwise decline of coral δ^{13}C has been reported and observed in the coral δ^{13}C dataset from the South China Sea[53] and Ogasawara[54] (Fig.S1). Coral δ^{13}C in Xisha Island coral step wisely declined $-0.26\permil$ for 1986–1988 and $-0.59\permil$ for 1997/1998. Coral δ^{13}C in Ogasawara coral also suggests the same decline trend as $-0.21\permil$ in 1976–1978 of El Nino years and $-0.65\permil$ in 1986–1988. These results suggest the decline of coral δ^{13}C is not only an event in southeast Taiwan but also a common regional event of the north-western Pacific.

The Kuroshio current intensified during the El Nino years; Kuroshio water intrusion increased to the northwestern Pacific[55]. The Kuroshio Current transports heat, tropical organisms such as reef-building corals, and fishery resources to high latitudes and is a carbon dioxide sink[56,57]. The Kuroshio Current and its successor basins are high carbon dioxide sinks cooled by the northward flow of water masses with low carbon dioxide partial pressures. The DIC δ^{13}C could cause the decline of coral δ^{13}C in El Nino years. Another possibility is that δ^{13}C of juvenile fish and zooplankton in the Kuroshio Current is about $-20\permil$[58], which is lower than the coral δ^{13}C ($-3.0\permil$ in this study). The coral δ^{13}C decreased after the 1997/1998 El Niño without changing the annual extension. The heterotrophic feeding also might compensate for the lack of photosynthetic energy due to the decrease in symbiotic algae[59].

This study found a decreasing shift in carbon isotope ratios of coral skeletons on Green Island, Taiwan, before and after the 1997/1998 El Niño event. This is thought to be the result of a rapid decrease in carbon isotope ratios due to bleaching, a decrease in symbiotic algae, and/or a change to heterotrophy high water temperature stress and in a continuous decrease in carbon isotope ratios in the DIC due to the Suess Effect. Although similar reports have been made in some areas, it will be necessary in the future to compare the occurrence of carbon isotope ratio declines in Porites corals in areas where bleaching events have occurred. In addition, clarifying the mechanism of carbon isotope ratio fluctuation itself may make it possible to use it as a more precise indicator of bleaching or as an indicator of rates in algal symbiosis.

Data availability
After publication, all coral data will be available on the data repository at the KIKAI Institute for Coral Reef Sciences (https://coralogy.kikaireefs.org).

References
1. Trenberth, K. E. & Hoar, T. J. El Ninõ and climate change. *Geophys. Res. Lett.* **24**, 3057–3060. https://doi.org/10.1029/97GL03092 (1997).
2. Goreau, T., McClanahan, T., Hayes, R. & Strong, A. Conservation of Coral reefs after the 1998 global bleaching event. *Conserv. Biol.* **14**, 5–15 (2000).
3. Brown, B. E. Coral bleaching: causes and consequences. *Coral Reefs* **16**, S129–S138. https://doi.org/10.1007/s003380050249 (1997).
4. Fitt, W. K., Spero, H. J., Halas, J., White, M. W. & Porter, J. W. Recovery of the coral *Montastrea annularis* in the Florida Keys after the 1987 caribbean bleaching event. *Coral Reefs* **12**, 57–64. https://doi.org/10.1007/BF00302102 (1993).
5. Grottoli, A. G. & Rodrigues, L. J. Bleached *Porites compressa* and *Montipora capitata* corals catabolize δ^{13}C-enriched lipids. *Coral Reefs* **30**, 687–692. https://doi.org/10.1007/s00338-011-0756-0 (2011).
6. Grottoli, A. G., Rodrigues, L. J. & Palardy, J. E. Heterotrophic plasticity and resilience in bleached corals. *Nature* **440**, 1186–1189. https://doi.org/10.1038/nature04565 (2006).
7. Porter, J. W., Fitt, W. K., Spero, H. J., Rogers, C. S. & White, M. W. Bleaching in reef corals: physiological and stable isotopic responses. *Proc. Natl. Acad. Sci. USA* **86**, 9342–9346. https://doi.org/10.1073/pnas.86.23.9342 (1989).
8. Rodrigues, L. J. & Grottoli, A. G. Energy reserves and metabolism as indicators of coral recovery from bleaching. *Limnol. Oceanogr.* **52**, 1874–1882. https://doi.org/10.4319/lo.2007.52.5.1874 (2007).
9. Barkley, H. C. & Cohen, A. L. Skeletal records of community-level bleaching in Porites corals from Palau. *Coral Reefs* **35**, 1407–1417. https://doi.org/10.1007/s00338-016-1483-3 (2016).
10. Mallela, J., Hetzinger, S. & Halfar, J. Thermal stress markers in *Colpophyllia natans* provide an archive of site-specific bleaching events. *Coral Reefs* **35**, 181–186. https://doi.org/10.1007/s00338-015-1350-7 (2016).
11. Cantin, N. E. et al. Ocean warming slows coral growth in the central Red Sea. *Science* **329**, 322–325. https://doi.org/10.1126/science.1190182 (2010).
12. Cantin, N. E. & Lough., J. M. Surviving coral bleaching events: *Porites* growth anomalies on the great barrier reef. *PLoS One* **9**, 1–12. https://doi.org/10.1371/journal.pone.0088720 (2014).

13. Hetzinger, C., Pfeiffer, M., Dullo, W. C., Zinken, J. & Garbe-Schönberg, D. A change in coral extension rates and stable isotopes after El Niño induced coral bleaching and regional stress events. *Sci. Rep.* **6**, 1–10. https://doi.org/10.1038/srep32879 (2016).

14. Nozaki, Y., Rye, D. M., Turekian, K. K. & Dodge, R. E. A 200 year record of carbon-13 and carbon-14 variations in a Bermuda coral. *Geophys. Res. Lett.* **5**, 825–828. https://doi.org/10.1029/GL005i010p00825 (1978).

15. Allison, N. & Finch, A. A. A high resolution $\delta^{13}C$ record in a modern *Porites lobata* coral: insights into controls on skeletal $\delta^{13}C$. *Geochim. Cosmochim. Acta* **84**, 534–542. https://doi.org/10.1016/j.gca.2012.02.004 (2012).

16. Swart, P. K., Leder, J. J., Szmant, A. M. & Dodge, R. E. The origin of variations in the isotopic record of scleractinian corals: II. Carbon. *Geochim. Cosmochim. Acta* **60**, 2871–2885. https://doi.org/10.1016/0016-7037(96)00119-6 (1996).

17. Grottoli, A. G. & Wellington, G. M. Effect of light and zooplankton on skeletal $\delta^{13}C$ values in the eastern Pacific corals *Pavona clavus* and *Pavona gigantea. Coral Reefs* **18**, 29–41. https://doi.org/10.1007/s003380050150 (1999).

18. McCounnaughey, T. ^{13}C and ^{18}O isotopic disequilibrium in biological carbonatepatternstterns. *Geochim. Cosmochim. Acta* **53**, 151–162. https://doi.org/10.1016/0016-7037(89)90282-2 (1989a).

19. McCounnaughey, T. $\delta^{13}C$ and $\delta^{18}O$ isotopic disequilibrium in biological carbonates: II. *In vitro* simulation of kinetic isotope effects. *Geochim. Cosmochim. Acta* **53**, 163–171. https://doi.org/10.1016/0016-7037(89)90283-4 (1989b).

20. Gagan, M. K., Chivas, A. R. & Isdale, P. J. Timing coral-based climatic histories using $\delta^{13}C$ enrichments driven by synchronized spawning. *Geology* **24**, 1009–1012 (1996).

21. Wang, C. et al. Super instrumental El Niño events recorded by a *Porites* coral from the South China Sea. *Coral Reefs* **37**, 295–308. https://doi.org/10.1007/s00338-018-1658-1 (2018).

22. Kajita, H. et al. Holocene sea surface temperature variations recorded in corals from Kikai Island, Japan. *Geochem. J.* **51**, e9–e14. https://doi.org/10.2343/geochemj.2.0482 (2017).

23. Li, X. et al. Trace of the 1997 Indonesian wildfires in the marine environment from a network of coral $\delta^{13}C$ records. *Geophys. Res. Lett.* **44**. https://doi.org/10.1029/2020GL090383 (2020).

24. Andrews, A. H., Asami, R., Iryu, Y., Kobayashi, D. R. & Camacho, F. Bomb-produced radiocarbon in the wetern tropical Pacific Ocean: Guam coral reveals operation-specific signals from the Pacific proving grounds. *J. Geoophys. Res. Oceans* **121**, 6351–6366. https://doi.org/10.1002/2016JC012043 (2016).

25. McCulloch, M. T., Gagan, M. K., Mortimer, G. E., Chivas, A. R. & Isdale, P. J. A high-resolution Sr/Ca and $\delta^{18}O$ coral record from the great barrier reef, Australia, and the 1982–1983 El Niño. *Geochim. Cosmochim. Acta* **58**, 2747–2754. https://doi.org/10.1016/0016-7037(94)90142-2 (1994).

26. Cheung, A. H. et al. Fidelity of the coral Sr/Ca paleothermometer following heat stress in the northern Garapagos. *Paleoceanogr. Paleoclimatol.* **36** (2021).

27. Mitsuguchi, T., Dang, P. D., Kitagawa, H., Uchida, T. & Shibata, Y. Coral Sr/Ca and Mg/Ca records in Con Dao Island off the Mekong Delta: assessment of their potential for monitoring ENSO and East Asian monsoon. *Glob. Planet Change* **63**, 341–352. https://doi.org/10.1016/j.gloplacha.2008.08.002 (2008).

28. Clarke, H., D'Olivo, J. P., Conde, M., Evans, R. D. & McCulloch, M. T. Coral records of variable stress inpamcts and possible acclimatization to recent marine heat wave events on the northwest shelf of Australia. *Paleoceanogr. Paleoclimatol.* **34**, 1672–1688. https://doi.org/10.1029/2018PA003509 (2019).

29. Meibom, M. et al. Distribution of magnesium in coral skeleton. *Geophys. Res. Lett.* **31**. https://doi.org/10.1029/2004GL021313 (2004).

30. Shirai, K. et al. Minor and trace element incorporation into branching coral *Acropora nobilis* skeleton. *Geochem. Cosmochim. Acta* **72**, 5386–5400. https://doi.org/10.1016/j.gca.2008.07.026 (2008).

31. Tanaka, K. et al. Response of *Acropora digitifera* to ocean acidification: constraints from $\delta^{11}B$, Sr, mg, and Ba compositions of aragonitic skeletons cultured under variable seawater pH. *Coral Reefs* **34**, 1139–1149. https://doi.org/10.1007/s00338-015-1319-6 (2015).

32. Clarke, H. et al. Differential response of corals to regional mass-warming events as evident from skeletal Sr/Ca and Mg/ ratios. *Geochem. Geophys. Geosyst.* **18**, 1794–1809. https://doi.org/10.1002/2016GC006788 (2017).

33. D'Olivo, J. P. & McCulloch, M. T. Response of coral calcification and calcifying fluid composition to thermally induced bleaching stress. *Sci. Rep.* **7**. https://doi.org/10.1038/s41598-017-02306 (2017).

34. D'Olivo, J. P. et al. Long-term impacts of the 1997–1998 bleaching event on the growth and resilience of massive Porites corals from the central Red Sea. *Geochem. Geophys. Geosyst.* **20**, 2936–2954. https://doi.org/10.1029/2019GC008312 (2019).

35. Cohen, A. L. & Gaetani, G. A. Ion partitioning and the geochemistry of coral skeletons: solving the mystery of the vital effect. *EMU Notes Mineral.* **11**, 377–397. https://doi.org/10.1180/EMU-notes.10.11 (2010).

36. Barkley, R. A. The Kuroshio Current. *Sci. J.* **6**, 54–60 (1970).

37. Sowa, K., Watanabe, T., Nakamura, T., Sakai, S. & Sakamoto, T. Estimation of uncertainty for massive *Porites* coral skeletal density. *JAMSTEC Rep. Res. Dev.* **16**, 31–39. https://doi.org/10.5918/jamstecr.16.31 (2013).

38. Schrag, D. P. Rapid analysis of high-precision Sr/Ca ratios in corals and other marine carbonates. *Paleoceanography* **14**, 97–102. https://doi.org/10.1029/1998PA900025 (1999).

39. de Villiers, S., Greaves, M. & Elderfield, H. An intensity ratio calibration method for the accurate determination of Mg/Ca and Sr/ Ca of marine carbonate by ICP-AES. *Geochem. Geophys. Geosyst.* **3**. https://doi.org/10.1029/2001GC000169 (2002).

40. Watanabe, T. K., Watanabe, T., Ohmori, K. & Yamazaki, A. Improving analytical method of Sr/Ca ratios in coral skeleton for paleo-SST reconstructions using ICP-OES. *Limnol. Oceanogr. Methods* **18**, 297–310. https://doi.org/10.1002/lom3.10357 (2020).

41. Okai, T., Suzuki, A., Kawahata, H., Terashima, S. & Imai, N. Preparation of a New Geological Survey of Japan Geochemical Reference Material; Coral JCp-1. *Geostand. Geoanal. Res.* **26**, 95–99. https://doi.org/10.1111/j.1751-908X.2002.tb00627.x (2002).

42. Paillard, D., Labeyrie, L. & You, P. Macintosh program performs time-series analysis. *Eos* **77**, 379. https://doi.org/10.1029/96EO00259 (1996).

43. Rodionov, S. N. A sequential algorithm for testing climate regime shifts. *Geophys. Res. Lett.* **31**, L09204. https://doi.org/10.1029/2004GL019448 (2004).

44. Advanced Very High Resolution Radiometer. http://iridl.ldeo.columbia.edu/SOURCES/.NOAA/.NCDC/.OISST/.version2/.AVHRR/.sst/

45. the Climate Explorer in the Royal. Netherlands Meteorological Institute. http://climexp.knmi.nl/selectindex.cgi?id=someone@somewhere

46. Shen, C. C. et al. The calibration of *D*[Sr/Ca] versus sea surface temperature relationship for *Porites* corals. *Geochim. Cosmochim. Acta* **60**, 3849–3858. https://doi.org/10.1016/0016-7037(96)00205-0 (1996).

47. Gagan, M. K. et al. Temperature and surface-ocean water balance of the Mid-holocene Tropical Western Pacific. *Science* **279**, 1014–1018. https://doi.org/10.1126/science.279.5353.1014 (1998).

48. Suzuki, A., Yukino, I. & Kawahata, H. Temperature-skeletal $\delta^{18}O$ relationship for *Porites* australiensis from Ishigaki Island, the Ryukyus, Japan. *Geochem. J.* **33**, 419–428. https://doi.org/10.2343/geochemj.33.419 (1999).

49. Abram, N. J., Webster, J. M., Davies, P. J. & Dullo, W. C. Biological response of coral reefs to sea surface temperature variation: evidence from the raised Holocene reefs of Kikai-Jima (Ryukyu Islands, Japan). *Coral Reefs* **20**, 221–234. https://doi.org/10.1007/s003380100163 (2001).

50. Swart, P. K. et al. The ^{13}C Suess effect in scleractinian corals mirror changes in the anthropogenic CO_2 inventory of the surface oceans. *Geophys. Res. Lett.* **37**, L05604. https://doi.org/10.1029/2009GL041397 (2010).

51. Quigley, K. M. et al. Symbioses are restructured by repeated mass coral bleaching. *Sci. Adv.* **8**. https://doi.org/10.1126/sciadv.abq8349 (2022).
52. D'Angelo, C. et al. Local adaptation constrains the distribution potential of heat-tolerant Symbiodinium from Persian/Arabian Gulf. *ISME J.* **9**, 2551–2560. https://doi.org/10.1038/ismej.2015.80 (2015).
53. Wang, X. et al. Super instrumental El Niño events recorded by a *Porites* coral from the South China Sea. *Coral Reefs* **37**, 295–308. https://doi.org/10.1007/s00338-018-1658-1 (2018).
54. Fellis, T. et al. Subtropical coral reveals abrupt early-twentieth-century freshening in the western North Pacific Ocean. *Geology* **37**, 527–530. https://doi.org/10.1130/G25581A.1 (2009).
55. Yamazaki, A., Watanabe, T., Tsunogai, U., Iwase, F. & Yamano, H. A 150-year variation of the Kuroshio transport inferred from coral nitrogen isotope signature. *Paleoceanography* **31**. https://doi.org/10.1002/2015PA002880 (2016).
56. Takahashi, T. et al. Global sea-air CO2 flux based on climatological surface ocean pCO2, and seasonal biological and temperature effects. *Deep-Sea Res. II* **49**, 1601–1622. https://doi.org/10.1016/S0967-0645(02)00003-6 (2002).
57. Midorikawa, T., Nemoto, K. & Kamiya, H. Persistently strong oceanic CO2 sink in the western subtropical North Pacific. *Geophys. Res. Lett.* **32**. https://doi.org/10.1029/2004GL021952 (2005).
58. Kobari, T. et al. Trophic sources and pathways of mesozooplankton and fish larvae in the Kuroshio and its neighboring waters based on stable isotope ratios of carbon and nitrogen. *Prog. Oceanogr.* **210**. https://doi.org/10.1016/j.pocean.2022.102952 (2023).
59. Grottoli, A. & Wellington, G. Effect of light and zooplankton on skeletal δ13C values in the eastern Pacific corals Pavona clavus and Pavona gigantea. *Coral Reefs* **18**, 29–41. https://doi.org/10.1007/s003380050150 (1999).

Acknowledgements

Author contributions

Ikeda wrote the manuscript text and created all figures. All authors reviewed the manuscript.

Declarations

Competing interests

The authors declare no competing interests.

Additional information

Supplementary Information The online version contains supplementary material available at https://doi.org/10.1038/s41598-024-74219-5.

Correspondence and requests for materials should be addressed to T.W.

Reprints and permissions information is available at www.nature.com/reprints.

Publisher's note Springer Nature remains neutral with regard to jurisdictional claims in published maps and institutional affiliations.